NATURAL COMPUTING APPLICATIONS ON DERMATOSCOPE IMAGES

Ioana DUMITRACHE[1], Alina-Elena SULTANA[2], Radu DOGARU[3], Diana PETRACHE[4]

Dermoscopy is a domain that involves visual analysis and the experience of doctors plays a great role in visual diagnosis. Reliable systems for automatic analysis and classification of dermoscopy images are useful for both doctors and patients. These systems are used to preprocess, process and evaluate images. This paper presents some alternative methods for these steps, which help developing time and space efficient systems with a higher degree of integrability. Our approach involves natural computing techniques that prove to give good results in this area. A parallel to results obtained with other methods is presented.

Keywords: natural computing, cellular automata, reaction-diffusion cellular nonlinear networks, image processing, classification, radial basis functions, automated dermatoscopy, voter model

1. Introduction

Malignant melanoma is a form of cancer with a very large incidence worldwide. Early detection is crucial in increasing the survival rate of patients and self-examination is the first step in detecting possible problems [1]. The diagnosis of melanoma is done through a biopsy; though, a preliminary evaluation can be performed using non-invasive techniques. Automated systems are meant to help clinicians give more accurate diagnosis [2].

There are three main steps in automated-diagnosis systems: 1. image acquisition; 2. feature extraction; 3. classification. In the second step a preliminary phase for image enhancement can be added, if necessary; this is done usually when artifacts are present. Some dermatoscope systems use for classification trained artificial neural networks, like single-layer perceptron [3] or self-

[1] PhD student, Research Assistant, Doctoral School on Electronics, University POLITEHNICA of Bucharest; National Institute for Laser, Plasma and Radiation Physics, Măgurele, Romania, e-mail: ioana.dumitrache2010@gmail.com

[2] Lecturer, Department of Applied Electronics and Information Engineering, University POLITEHNICA of Bucharest, Romania

[3] Professor, Department of Applied Electronics and Information Engineering, University POLITEHNICA of Bucharest, Romania

[4] Doctor, MedLife Unirii Clinic, Bucharest, Romania

generating neural networks using a genetic algorithm for seeding [4]. Studies for artifact removal and data classification are done in [5, 6].

Specialists in the domain [1-5, 7-9] present four major visual characteristics of nevi that have to be considered in the examination of the skin lesion, generically named the ABCD rule: asymmetry (A), border irregularity (B), color (C), diameter larger than 5-6 millimeters and / or growing if followed one month (D). Without information on magnification or evolution in time, the diameter is not used as feature; in order to simplify the method, only the intensity level is considered, not all color components.

Natural computing refers to technical methods inspired by different systems found in nature that prove to be very efficient in solving some problems [10]. Considering the performance, one of the most complex and interesting systems is the human brain. Haykin defines the brain as a "highly complex, nonlinear and parallel computer" [11]. The proposed methods are based on cellular automaton and reaction-diffusion cellular nonlinear network paradigms.

Wolfram [12] describes cellular automata (CA) as a collection of identical cells with similar behavior, each site having a finite set of values and interacting with a number of neighbors. The system is discrete [13] and has a temporary evolution that begins at a moment, t_0, when the network is initialized; the state of a cell at the moment t_n depends on the state of the same cell and its defined neighbors at the previous moment, t_{n-1}.

In [14] cellular automata are used to extract handwritten character features for character recognition. The system presented implements a 2D, semi-totalistic, von Neumann architecture that leads, after a number of iterations, at building a bounding box around each character (using a binary image). The technique used for character recognition proves to be useful in other imaging applications also.

Chua and Yang introduce the paradigm of "cellular neural networks" (CNNs) [15] as a combined model of neural networks and cellular automata, a continuous time nonlinear system consisting of interconnected cells that communicate only with neighbors in immediate proximity, allowing real-time signal processing. A cell is described by a set of variables: input, state, initial state, output [16]. Examples of ordinary differential equations (for continuous time) or difference equations (discrete time) are presented in [16] for the temporal evolution of the system. The concept of "gene" is introduced to describe the entire set of parameters defining the function used in the equations used to draw the evolution of the system. A multi-layer CNN inspired from physical concepts of reaction and diffusion is presented in [16, 17]. It is convenient implementing it as a resistive grid on multiple levels; hence, it is named "reaction-diffusion cellular nonlinear network" (RD-CNN). The term "reaction" is used to express the relation between layers, while "diffusion" refers to the signal communicated between neighbor cells. Having a network with m layers and defining, for each cell an n-

neighborhood in continuous time, a generalized form of the equation of a cell presented in [16] can be described as:

$$\dot{x}_1^k = f_1(x_1^1, x_1^2, ..., x_1^k, G_k) + D_k(x_2^k + x_3^k + ... + x_n^k - nx_1^k) \quad (1)$$

where k=1…m (number of layers); x_1^k is the generic considered cell on layer *k*, $x_2^k, ..., x_n^k$ it's neighbors, G_k the gene used on layer k and D_k the diffusion coefficient on layer *k*. The discretized form is presented in [13], and can be expressed generally as:

$$x_1^k(t+1) = x_1^k(t) + dt(f_1(x_1^1(t), x_1^2(t), ..., x_1^k(t), G_k)) + D_k(x_2^k(t) + x_3^k(t) + ... + x_n^k(t) - nx_1^k(t))) \quad (2)$$

Eq. (2) uses the same notations as eq. (1), adding the temporal dependence; the state of the cells at moment *t+1* is influenced by the state of the cells at the previous moment *t*. The final result of the processing depends on the number of iterations; the number of iterations multiplied by *dt* represents a period in continuous time.

The paper is organized as follows: Section 2 introduces the general principles employed by our method and presents the processing flow. Section 3 gives details on specific stages of the image processing where various natural computing methods were employed. In Section 4 specific details are given on how feature vectors associated with the input image are generated. Such labeled feature vectors are the basis for training certain classification systems, as discussed in Section 5, where the overall performance of our method is evaluated on our database.

2. Proposed approach

The purpose of this work is to give an approach on how different natural computing techniques can be used in a digital melanoma recognition system. The focus is on image enhancement by artifacts removal; results are compared to those presented in [5]. Extracted features are used to train and test a radial-basis function classifier [6] and the SVM classifier from Matlab toolbox.

A proprietary database with labeled samples of nevi is constructed and still in progress as part of our research. It consists of dermoscopy images acquired and evaluated by a specialist; the labels are healthy (28 images) and suspect (23 images). Although, at this moment the size of our database is still small, since no other publicly databases were found until now, it is extremely useful in assessing and comparing various methods and for optimizing their parameters. It also

allows finding the most appropriate features to be used in the classification process. The examined nevi are coming from fair-skinned persons and are melanocytic (they are pigmented). This feature can be useful in delimitating it by applying an intensity threshold on the image. This could be an efficient and quick processing step if images would show only the skin and the lesion, but the color information can be influenced by artifacts such as black frame and hair. Note that a black region (called "black frame") appears near the margins of the pictures, usually in the corners, but sometimes even as a clear circle around the examined area (Fig. 1).

a) b)

Fig. 1 Artifacts in dermatoscopy images: a) black frame at the corners of the image, decreasing in intensity on the inside part; dark, thick hair; b) very dark and prominent black frame, few thin hair patterns.

In order to extract features from dermoscopy images, a clear segmentation of the nevi needs to be done, with as few artifact traces as possible. The focus here is on techniques within the natural computing area.

For the purpose of this work, the normalized intensity values of an image are used as initial state; hence, a 2-dimensional network is needed. Considering both RD-CNN and CA, the size of the network is proportional to the number of pixels of the processed image. For RD-CNN the functions defining the reaction are given by Fitz-Hugh Nagumo model, employing a 2-layered network (Fig. 2) [12, 13]:

$$f_1(x^1, x^2) = \alpha x^1 - (x^1)^3/3 - x^2 \tag{3}$$

$$f_2(x^1, x^2) = -\varepsilon(x^1 - bx^2 + a) \tag{4}$$

In Eq. (3) and (4) x^1 and x^2 are the states associated with the two layers, and the gene has four variables, namely a, b, ε, α. For each processing, a suitable gene must be experimentally found; in addition, the two diffusion coefficients must also be experimentally determined. A cell is characterized by its activity and stability, depending on the employed gene: some genes, those that lead to not active cells, do not alter the input signal and no useful processing is expected. A local activity map can be designed allowing to roughly locate these genes [18].

Two of the four variables are fixed, while the other two are defined between intervals; there are multiple classes of local activity, from which the most promising is the one defined as "edge of chaos", both active and stable. A detailed presentation of how the activity / stability areas are determined can be found in [18]; the information proves to be very useful not only to avoid passive behavior, but also to classify the other possible regions from most to least likely to be useful.

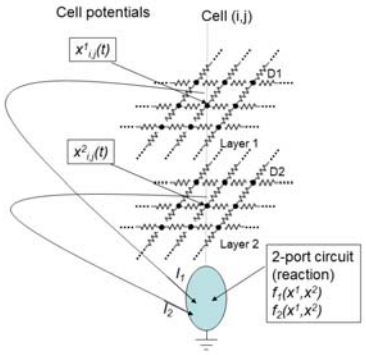

Fig. 2. The structure of a Reaction-Diffusion nonlinear network with *2* layers

The last step is the classification of the images. SVM is widely recognized as one of the best classifiers; however, as shown in [6], for some problems, other classifiers return better classification results on the test database. A classification using a modified model of radial basis function classifier (RBF-M) [6] is considered, these classifiers having also some good properties for further implementation of the automatic recognition system as an embedded system. Usually, the performance of a classifier is evaluated through the test database; the aim is to obtain the smallest classification error on the test database. For the purpose of a medical diagnosis, another criterion is also considered: the number of suspect nevi recognized by the system as healthy, a good system must reduce it to minimum. A diagram of the proposed approach is presented in Fig. 3.

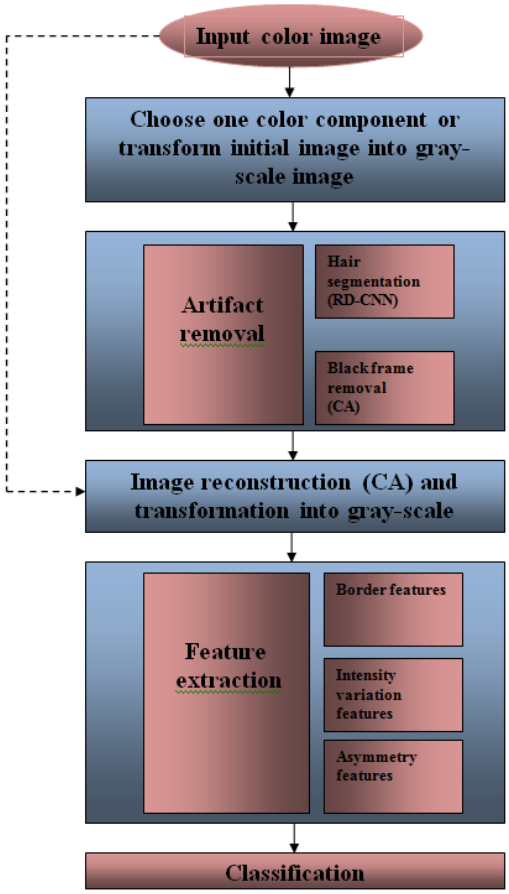

Fig. 3. Diagram of the proposed approach

3. Preprocessing and processing dermatoscopic images using natural computing techniques

Basic image preprocessing and processing, like binarization, segmentation or edge extraction have been employed long time using classical techniques and have proved to be very useful in feature extraction necessary for classification of the images. More elaborated computations, as hair and black frame removal are presented in [5]. Some alternative methods suitable for other hardware implementation, using natural computing techniques, are given in the following. Some operations have been previously presented in [19] and [20].

3.1 Applications of RD-CNNs on dermoscopy images

Previous results using RD-CNNs on dermatoscopic images, like binary segmentation, edge extraction or hair segmentation were shortly presented in [20]. For image enhancement hair removal is essential and in the following some issues regarding this step are addressed; a comparison with another method is done.

Hair segmentation

Hair represents one of the main artifacts in dermatoscopic images; similar to the black frame, they are darker and cannot be eliminated by thresholding. In image improvement and not only, hair reduction can be useful. Previous results were presented in [20], however they are more detailed here, and a comparison with another method is made. Experiments have shown that certain RD-CNNs genes have the effect of increasing the contrast regions in images. They can be used to do a segmentation of dark regions with a certain level of contrast relatively to the surroundings. Hair patterns are usually darker than the rest of the skin and, depending on the lesion's color, the nevi itself. Some genes prove to be useful in hair segmentation; after the transformation, an appropriate threshold for final binary result can be found much easier, as it can be observed in Fig. 4 and Fig. 5.

a) b)

Fig. 4 Hair segmentation using RD-CNNs; a) initial image; b) extracted hair patterns after binarization

In Fig. 4, b) can be seen the segmented hair from the initial image, shown Fig. 4, a); this mask is obtained after 500 iterations, using an "edge of chaos" gene, [-0.49 1.48 -0.1 1], and the diffusion coefficients 0.1 on the first layer and 1.8 on the second. The output result, here coming from the second layer of the RD-CNN network is binarized with a threshold considered appropriated for this purpose; the result obtained with the same gene and a lower threshold can be found in [20]. Usually this type of artifact has some particular traits: it is thinner and darker compared to other objects in the image. Considering these properties, a method for extracting hair is the top hat transform [5]; a comparison between the results of the two techniques is presented in Fig. 5.

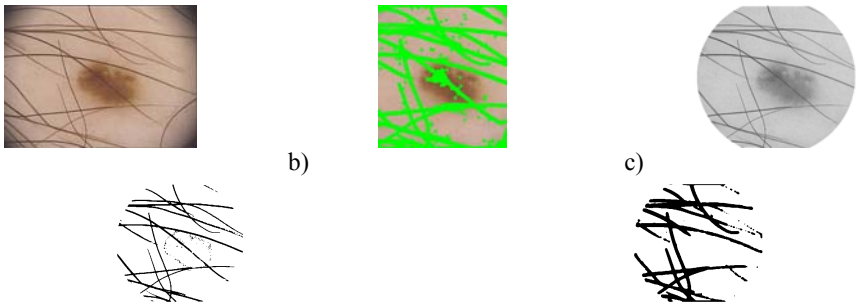

a) b) c)

d) e)

Fig. 5 Hair masks: a) original image using b) top-hat transform; c) original image without black frame and in intensity levels; d) RD-CNN, after 75 iterations, using a gene from "three points of unstable equilibrium" area; e) RD-CNN, after 200 iterations, using an "edge of chaos" gene.

Fig. 5 d) and e) show two different hair masks of the same input image. Below, the effect of eliminating segmented hair from the image can be seen (Fig. 6).

a) b)

Fig. 6. Hair mask applied on image in Fig. 5 c) using a) mask in Fig. 5, d); b) mask in Fig. 5, e).

Both situations in Fig. 6 present flaws, but the advantages make them useful in different further processing. In Fig. 6, a) a full extraction of the hair is performed, but some pixels near the edge of the lesion are eliminated too; also, the lesion is practically divided into two distinct parts. If this type of image is preferred for color or intensity analysis, it is less useful than Fig. 6, b) when doing an investigation of the borders.

When it comes to employing genes that lead to this type of behavior (contrast enhancement), Fig. 4, a) and 5, c) represent two distinct cases. In the first image the intensity of the hair is much higher than the lesion's, but in the second they are quite similar. By using the same gene as in Fig. 4 and the same number of iterations, hair outside the nevi is much better retrieved in Fig. 5, c), but the portion covering the lesion is hard to retrieve, even after a small number of iterations (Fig. 5, e)). A slightly different evolution is given by the gene used for obtaining Fig. 5, d), when the contrast hair-nevi is increased during the first iterations, followed by an abrupt decrease after maximum is reached in the region of interest. If a full recovery of the hair is wanted, the challenge here is to stop the evolution of the system when optimum is reached.

3.2 Cellular automata applied in dermatoscopic image processing

Black frame elimination using cellular automata

A method for character recognition using cellular automata is described in [14]. Around each number a rectangular bounding box is grown using a cellular automata, then features are extracted for classification. The geometric properties of the black frame are considered: the interior edge of the black frame is a circle or part of it. If a bounding box is built around the skin, the intersection of its diagonals is close to the center of the circle, making it easy to delimitate. Since the gene for bounding box used in [14] surrounds dark objects, a "negative" of the initial gray scale image is previously determined. The images are then binarized, to have the skin as a black object (intensity 0) and the rest as white (intensity 255).

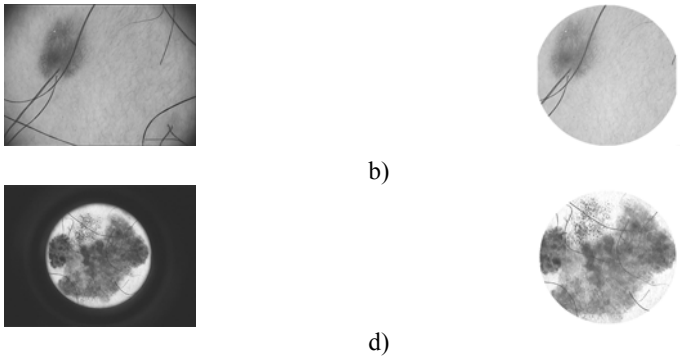

a) b)

c) d)

Fig. 7. Automatic black frame elimination

An issue of this method is choosing the same binarization threshold for all images in the dataset. This could lead to optimal results such as Fig. 7, a), or to a thin surrounding circle. This is because the nevi is too large and the black frame has a color similar to the one of the skin lesion. A solution to this problem is to have an interactive system, where the user can specify the threshold (Fig. 7, b)).

For the same problem (black frame elimination), a geometry-based method is used in [5], where the radius if the circle is increased until it reaches the black frame, and results are similar to those obtained through out method. Still, the use of cellular arrays with programmable genes has the advantage of flexibility over other methods. It is enough to change the gene in order to obtain different image processing effects. Consequently, a simple implementation can be obtained, which is an important aspect, when such automated systems have to be implemented in portable, embedded devices (such as mobile devices, etc.).

Replacement of missing regions

In literature there are presented several methods that employ cellular automata to fill missing parts in images, like flood filling [21] or parity control, improved by seed cell [22]. Although they seem promising for filling binary images, like those used for unique contour detection, they require the presence of a closed contour. The method that proved to be more appropriate to our needs is the one proposed in [23] for missing data in landscapes, employing the voter model. A previous similar landscape study is presented in [24]; both methods suggest the efficiency of a radial neighborhood as being optimal for clustering in landscape images. The method presented in [23] consists in defining a circular neighborhood for a missing cell and replacing it with a random neighbor. The main advantage of this method is that it does not affect the other pixels of the image.

The principle, that can be applied here too, is that the probability is higher for a pixel to have a similar value to a close pixel than to a distant one. A slightly different approach is used here. Since it is more likely to have multiple small regions missing than a big one, the number of neighbors does not need to be large and a circle neighborhood could be replaced by a square one for simplicity. Fig. 8 shows the enhancement effect of this model. In the following the neighborhood is expressed either as the distance from the line / column of the central pixel to the furthest line / column or as a matrix; hence, a neighborhood of 2 is equivalent to a neighborhood of 5x5.

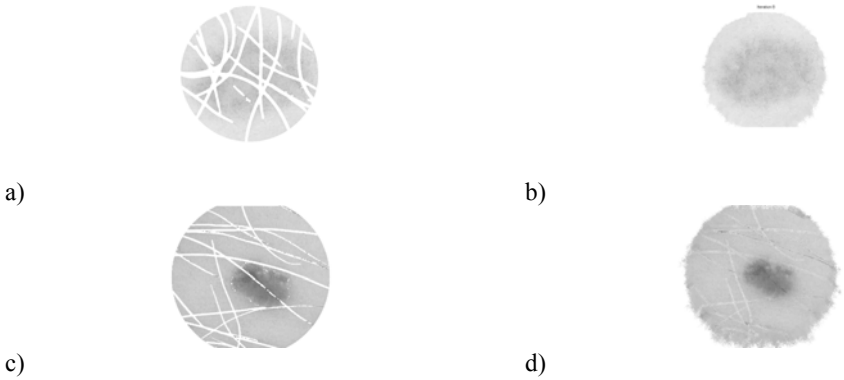

Fig. 8. Filling missing regions left after hair extraction; a) image with dramatic hair reduction; b) result obtained after filling missing parts in a); c) image with thinner marks left from hair reduction and; d) result of the filling

The results prove to be satisfactory after a small number of iterations, even for a dramatic presence of artifacts, like the one in Fig. 8, a) and c). The hair reduction in Fig. 8, c) is less optimal, but this is mainly observed on the skin. The

results on the main object in the image (the lesion) are acceptable, as seen in Fig. 8, d). For both cases presented previously, a full recovery was performed in less than 10 iterations.

In dermatoscopic images patterns represent a very important aspect; in order to see the effect of this model on the overall aspect of the lesion, an image with clear pattern was artificially modified and enhanced. The results after 6 iterations, using a neighborhood of 5x5 are shown in Fig. 9.

a) b) c)

Fig. 9. Missing pattern replacement: a) initial image; b) image with artificial artifacts; c) obtained image

A computational evaluation of the accuracy of the method is done by comparing the expected result and the obtained result from two points of view: 1) the number of pixels that differ between the two images and 2) the difference in intensity between the two images. The evaluation is done on gray-scaled images, Fig. 10. The error evolution on 100 iterations for a neighborhood between 1 and 10 is presented in Fig. 11 and 12.

a) b)

Fig. 10. Images used for error evaluation: a) "ideal" output; b) image with artificial artifacts

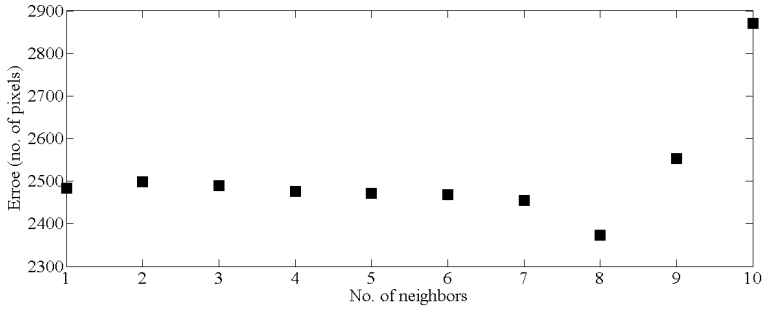

Fig. 11. Evolution of the number of pixels that differ in intensity between "ideal" output and obtained output

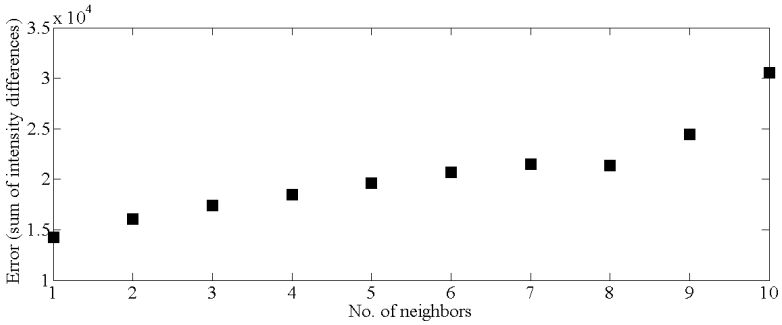

Fig. 12. Intensity difference between "ideal" and obtained output summated; evolution depending on the neighborhood size

For a better accuracy, since the gaps are filled randomly, the error is averaged on 100 repetitions. As expected, in both situations, the evolution of the error depending on the number of neighbors shows that a smaller neighborhood leads to better results. A local minimum in both cases is found around a neighborhood of 8.

A relative estimation of the error gives us a qualitative measure of the result. The number of white pixels in Fig. 10 b) is 5236 and for the optimal case, the number of pixels with a different color than the expected one is around 2350, meaning that about 45 % of the pixels were correctly determined. If the total difference between the "ideal" and the obtained image is approximated to 13000, the mean error per pixel is less than 6 out of 256 possible intensity levels of grey that the image used has, so the average intensity error per pixel is around 2.5 %, for this image.

Signature centroid

The same method presented previously and used in [14] can be applied to define the centroid of the skin nevi, also used as reference point for the signature [25] of the skin lesion in the image. This is particularly useful if the lesion is not centered on the image. The cellular automata model presented in [14] and previously used in [19] allows us to build a bounding box around the nevi, and the diagonals intersection of this rectangle is considered the centroid of the nevi.

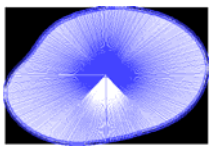

Fig. 13. Example of bounding box and signature around an object

4. Feature extraction

Image retrieval and classification is based on finding similar features or elements that can differentiate images. An useful tutorial on how the ABCD rule is applied is found in [26] and the rules presented there are used as guidelines.

Features extracted from images (based on the signatures determined as above) cover asymmetry, border irregularities and intensity variations. For classification both the classical SVM and a modified radial basis function classifier presented in [23] proved to be more accurate in some situations, were used.

Using the signature, the largest diameter is found and used as a main axis, the second main axis being its perpendicular. Two vectors that give a measure for border asymmetry along each axis are determined (ASYMB1, ASYMB2). In these datasets, clustering to a certain degree can be observed, but also regions of intersection. For border irregularity the parameters used in [19] were Lyapunov exponents, giving a measure of the chaos degree in a vector (LV). Also, a parameter that improved the results was the ratio between the largest and the smallest diameters of the lesion (DIAMRATIO).

The intensity variations from center to the edges and abrupt changes are done in five points along eight axes at 45 degrees; the five points represent the central point of a matrix. In order to detect large variations of intensity, the difference between two successive points are used, and the maximum along an axis retained in the end (COLVAR). Another way to measure intensity variations is inspired by the character recognition model [14]. The bounding box is constructed around a segmented nevi (the background is white); then, it is divided vertically and horizontally into m*n sub-matrices. The average intensity of each sub-matrix is computed, excluding white pixels (background), resulting an m*n matrix. For determining color variations, the features vector consists in the difference between each to neighbor cells of the matrix, taking a von Neumann neighborhood. The result is a vector with dimension (m-1)*n+m*(n-1) - FCOL.

5. Classification results and discussion

In this section the features extracted in section 4 are tested in order to see if they can be used in an automatic diagnosis tool. These attributes were extracted after the preprocessing step in order to have a numeric characterization of the nevi as accurate as possible. As mentioned in section 2, the image database contains 51 images, divided in two classes, healthy (28 images) and suspect (23 images). For evaluating the accuracy of the extracted features two classifiers that work on the principle of supervised learning are used: SVM and RBF-M. In this purpose the database is divided in two parts, one used for training the classifiers and the other to test them. Each test image is automatically assigned to one of the two classes,

healthy or suspect. It is expected that the assigned class corresponds to the initial label given by the dermatology specialist. The performance is computed considering the classification results on the test database compared to the expected ones: the percentage of correctly assigned images from the total test database. Opposite to the performance (accuracy) is computed the relative error, as the percentage of misclassified images from the total test database (eq. 5). Another factor considered is the percentage of misclassified suspect nevi, that must be minimized (the calculation is analogue to eq. 5).

$$error[\%] = \frac{no\_of\_misclassified\_test\_images}{no\_of\_test\_images} * 100 \quad (5)$$

Each feature presented in the previous section is used individually to train the two classifiers; the other features are gradually added until an optimum classification result is obtained. The features cover asymmetry of borders (ASYMB1, ASYMB2), border irregularity (LV), circularity (DIAMRATIO) and intensity variation (COLVAR, FCOL).

For the classification experiments the database is divided into two parts, the first one consisting in 20 images (10 healthy randomly chosen and 10 suspect also randomly chosen) – DB20 and the other in the rest of 31 images (18 healthy, 13 suspect) – DB31. Both subdivisions are used alternatively for training and testing the two classifiers. The best outcome from each classifier is presented.

A compromise between the general relative error and the relative error on the suspect part of the test database.

In Table 1 the best outcomes from the two classifiers are summarized.

Table 1

Classification results using SVM and RBF-M

Classifier	SVM	RBF-M
Training Database	DB20	DB31
Training database dimension	20 images	31 images
Test database dimension	31 images	20 images
No. of healthy images for test	18	10
No. of suspect images for test	13	10
No. of feature vectors used	4	2
Feature vectors	COLVAR DIAMRATIO ASYMB1 ASYMB2	LV FCOL
No. of misclassified images	7	4
No. of misclassified suspect images	1	0
Misclassification rate	23 %	20 %

A number of factors influence the results presented in Table 1:

- The chosen features and methods through which the features were extracted – these features were computed according to visual analysis indications; more advanced mathematical procedures might be useful in their improvement;
- The reconstruction accuracy part depends on the segmentation accuracy, on the nature of the image and on the optimal choice of the neighborhood;
- The small number of images.

However, the performance is promising, especially for a system that aims not only the diminution of the error, but also the increase of the integration degree by using architectures like RD-CNN, CA and RBF-M. These natural computing approaches offer the possibility to create algorithms adaptable to other types of architectures, parallel and more integrated.

6. Conclusion

Natural computing alternatives to classical methods for dermoscopy image processing and classification were presented. Also, due to the nature of the artifacts and the structure of the images, a simplified model for enhancement can be used. These methods return promising results for both processing and classification; they exhibit low computational complexity making them suitable for integration of automatic detection algorithms (including image enhancing that are preliminary to feature computing and classification) into embedded dermoscopy systems.

Acknowledgments

The work has been funded by the Sectoral Operational Programme Human Resources Development 2007-2013 of the Ministry of European Funds through the Financial Agreement POSDRU/159/1.5/S/132397.

R E F E R E N C E S

[1]. *D. S. Rigel, J. A. Carucci*, “Malignant melanoma: Prevention, early detection, and treatment in the 21st century”, CA: A Cancer Journal for Clinicians, **Vol. 50**, Issue 4, pp. 215-236, July/August 2000

[2]. *D. Piccolo, A. Ferrari, K. E. T. T. Y. Peris, R. Daidone, B. Ruggeri, and S. Chimenti.* "Dermoscopic diagnosis by a trained clinician vs. a clinician with minimal dermoscopy training vs. computer-aided diagnosis of 341 pigmented skin lesions: a comparative study." British Journal of Dermatology **Vol. 147**, no. 3 (2002): 481-486

[3]. *P. Rubegni, M. Burroni, G. Cevenini, R. Perotti, G. Dell'Eva, P. Barbini, M. Fimiani, and L. Andreassi*. "Digital dermoscopy analysis and artificial neural network for the differentiation of clinically atypical pigmented skin lesions: a retrospective study." Journal of investigative dermatology **Vol. 119**, no. 2 (2002): 471-474; doi:10.1046/j.1523-1747.2002.01835.x

[4]. *F. Xiea, A. C. Bovikb*, "Automatic segmentation of dermoscopy images using self-generating neural networks seeded by genetic algorithm", Pattern Recognition, **Vol. 46**, Issue 3, March 2013, Pages 1012–1019

[5]. *A. Sultana, I. Dumitrache, M. Vocurek, and M. Ciuc*. "Removal of artifacts from dermatoscopic images." In Communications (COMM), 2014 10th International Conference on, pp. 1-4. IEEE, 2014., doi: 10.1109/ICComm.2014.6866757

[6]. *R. Dogaru*, "A hardware oriented rbf classifier with simple constructive training based on support vectors", Proceedings of CSCS-16, the 16th International Conference on Control Systems and Computer Science, May 22 - 26, 2007, Bucharest, Romania, **Vol.1**, pp. 415-418, ISBN 978-973-718-741-3.

[7]. *** American Cancer Society: Cancer Facts and Figures 2013. Atlanta, Ga: American CancerSociety, 2013

[8]. *A. Sultana, M. Ciuc, T. Radulescu, L. Wanyu, and D. Petrache*, "Preliminary Work on Dermatoscopic Lesion Segmentation", 20th European Signal Processing Conference (EUSIPCO 2012), Bucharest, Romania, August 27-31, 2012

[9]. *D. S. Rigel et al.*, "Dysplastic Nevi Markers for Increased Risk for Melanoma", CANCER, January 15, 1989, **Vol. 63**, pp. 386-389

[10]. *L. Kari, G. Rozenberg*, "The many facets of natural computing", Communications of the ACM **51** (10), 72-83, 2008

[11]. *S. Haykin*, "Artificial Neural Networks: A Comprehensive Foundation", Second Edition, Pearson Education, 1999

[12]. *S. Wolfram*, "A new kind of science", Wolfram Media Inc., Champaign, Ilinois, US, 2002

[13]. *J. Gorodkin et al.*, "Neural Networks and Cellular Automata Complexity", Complex Systems **Vol. 7** (1993), pp. 1-23, 1993

[14]. *R. Dogaru, I. Dogaru, and M. Glesner*, "A smart sensor architecture based on emergent computation in an array of outer-totalistic cells", Bioengineered and Bioinspired Systems II, edited by Ricardo A. Carmona, Gustavo Liñán-Cembrano, Proceedings of SPIE **Vol. 583**, pp. 254-263

[15]. *L. Chua and L. Yang*, "Celular Neural Networks: Theory", IEEE Transactions on Circuits and Systems, **Vol. 35**, No. 10, October 1988

[16]. *R. Dogaru*, "Systematic Design for Emergence in Cellular Nonlinear Networks", Chapter 3 – "Cellular and natural computing models and software simulations", Springer, 2008

[17]. *R. Dogaru*, "Applications of Emergent Computation in Reaction-Diffusion CNNs for Image Processing," 2013 19th International Conference on Control Systems and Computer Science (CSCS), pp.370-377, 29-31 May 2013 doi: 10.1109/CSCS.2013.39

[18]. *R. Dogaru*, "Universality and Emergent computation in Cellular Neural networks", Ch. 4, "Emergence in Continuous-Time Systems: Reaction-Diffusion Cellular Neural Networks", World Scientific Series on Nonlinear Science, Series A, **Vol. 43**, 2003

[19]. *Ioana Dumitrache, Alina Sultana, Radu Dogaru*, "Automatic detection of skin melanoma from images using natural computing approaches", 10th International Conference on Communications (COMM), pp.1,4, 29-31 May 2014, doi: 10.1109/ICComm.2014.6866748

[20]. *I. Dumitrache, A. Sultana, R. Dogaru*, "Reaction-diffusion cellular nonlinear networks for feature enhancement in dermatoscopic images," 2013 4th International Symposium on Electrical and Electronics Engineering (ISEEE), pp.1-4, 11-13 Oct.2013, doi:10.1109/ISEEE.2013.6674314

[21]. *P. Rosin, A. Adamatzky, and X. Sun*, "Cellular automata in image processing and geometry", **Vol. 10**, Springer, 2014, pp. 155

[22]. *S. Bilan*, "Models and hardware implementation of methods of pre-processing images based on cellular automata", AIVP, **Vol. 2**, Issue 5, October 2014, pp. 76-90

[23]. *J. C. Sprott*, "A method for approximating missing data in spatial patterns", Computer & Graphics **28**, 2004, pp. 113-117

[24]. *J. Bolliger, J. C. Sprott, and D. J. Mladenoff*, "Self-organization and complexity in historical landscape patterns", OIKOS 100, **3**, 2003, pp. 541-553

[25]. *R. Dogaru, I. Dogaru*, "An efficient finite precision RBF-M Neural Network architecture using support vectors", 10th Symposium on Neural Network Applications in Electrical Engineering, Serbia, 2010

[26]. http://www.dermoscopy.org/consensus/2b.asp